Journal of Peptide Science
J. Peptide Sci. **9**: 229–243 (2003)
Published online in Wiley InterScience (www.interscience.wiley.com). DOI: 10.1002/psc.449

JOURNAL OF PEPTIDE SCIENCE

Conformational Features of a Synthetic Model of the First Extracellular Loop of the Angiotensin II AT_{1A} Receptor

GIUSEPPE NICASTRO,[a] FRANCESCO PERI,[b] LORELLA FRANZONI,[a] CESIRA DE CHIARA,[a] GIORGIO SARTOR[a,†] and ALBERTO SPISNI[a]*

[a] Department of Experimental Medicine, Section of Chemistry and Structural Biochemistry, University of Parma, 43100 Parma, Italy
[b] Department of Biotechnology and Biosciences, University of Milano-Bicocca, 20126 Milano, Italy

Received 12 September 2002
Accepted 30 October 2002

Abstract: The angiotensin II AT_{1A} receptor belongs to the G-protein coupled receptors (GPCRs). Like other membrane proteins, GPCRs are not easily amenable to direct structure determination by the currently available methods. The peptide encompassing the putative first extracellular loop of AT_{1A} (residues Thr^{88}-Leu^{100}, el1) has been synthesized along with a cyclic model where the linear peptide has been covalently linked to a template designed to keep the distance between the peptide termini as expected in the receptor. The conformational features of the two molecules have been studied using circular dichroism and NMR techniques. The region $W^{94}PFG^{97}$ forms a type-II β-turn and undergoes a Trp-Pro peptide bond *cis-trans* isomerization in both peptides confirming that these characteristics are intrinsic to el1. In addition, the presence of the spacer seems to modulate the flexibility of the peptide. Copyright © 2003 European Peptide Society and John Wiley & Sons, Ltd.

Keywords: angiotensin II; circular dichroism; NMR; peptide mimetic; G-protein coupled receptor

INTRODUCTION

GPCRs modulate several physiological and pharmacological events. In spite of their biological relevance, a clear comprehension of many aspects of their function–structure relationship is hampered by the limited structural data available. Though the crystal structure of rhodopsin [1] and of the metabotropic glutamate receptor with and without the ligand [2] have been recently determined and several models of GPCRs have been proposed [3–11], not much is known of the structural features of the extracellular and intracellular loops.

Mutagenesis and biophysical analysis of a number of GPCRs revealed a differentiation between the binding sites for peptides and small molecules [12–15]. While small agonists and/or antagonists bind to hydrophobic sites buried inside the transmembrane core of the receptor, larger molecules such as peptides, bind to both extracellular

Abbreviations: Boc, *tert*-butoxycarbonyl; tBu, *tert*-butyl; CD, circular dichroism; COSY, correlation spectroscopy; CVFF, consistent valence force field; Dde, 1-(4,4-dimethyl-2,6-dioxocyclohexylidene)ethyl; DMF, N,N-dimethylformamide; DSS, 4,4-dimethyl-4-silapentane-1-sulfonate; el1, first extracellular loop of the AT_{1A} receptor; el1-KG-NH_2, TAMEYRWPFGNHLKG-NH_2; Fmoc, 9-fluorenylmethyloxycarbonyl; GPCRs, G-protein coupled receptors; MeOH, methanol; NOESY, nuclear Overhauser enhancement spectroscopy; Pmc, 2,2,5,7,8-pentamethylchroman-6-sulfonyl; TFA, trifluoroacetic acid; TFE, 2,2,2-trifluoroethanol; TIS, *tris*-isopropylsilane; TOCSY, total correlation spectroscopy; Trt, trityl or triphenylmethyl.

* Correspondence to: Dr Alberto Spisni, Dipartimento di Medicina Sperimentale, Sezione di Chimica e Strutturistica Biochimica, Università di Parma, Via Volturno 39, 43100 Parma, Italy;
e-mail: aspin@unipr.it
† Present address: Interdepartment Centre for Environmental Science Research, University of Bologna, 48100 Ravenna, Italy.
Contract/grant sponsor: CNR; Contract/grant number: 99.02608.-CT04.
Contract/grant sponsor: MIUR.

and transmembrane domains [14,16]. Indeed, the involvement of extracellular domains in peptide binding has been demonstrated for several GPCRs classes, including those of the C5a complement cleavage product, formyl-methionyl-leucyl-phenylalanine, neurokinin-1, bradykinin and angiotensin [12,13,17–22].

In the case of the angiotensin II AT_{1A} receptor, mutational studies have indicated that some residues located in the first, second and third extracellular loops (el1, el2 and el3) are essential for agonist binding [23–27]. As for el1, while its precise sequence extension is not yet clear, there is evidence that Tyr^{92} plays a crucial role in this process [23]. In addition, it is worth pointing out that residue Tyr^{92}, together with the sequence $W^{94}PFG^{97}$ and Cys^{101}, all belonging to the same loop, are highly conserved in various species [12,28].

The study of the conformational features of segments spanning functional regions of these large membrane proteins has turned out to be a useful method both to explain some aspects of their functionality in the whole receptor [29–42] and to devise more reliable molecular models of the whole native protein [43–45].

Our previous studies on the peptide Y^{92}RWPF-$GNHL^{100}$, (*f*el1), used as a possible model of el1 of the AT_{1A} receptor, suggested that, while in aqueous solution the peptide is in equilibrium between various conformations, in viscous systems it forms a β-turn, involving residues $W^{94}PFG^{97}$, where the Trp-Pro peptide bond undergoes a *cis-trans* isomerization [46,47].

In order to verify whether the conformational properties, observable only in specific media, are intrinsic features of that polypeptide chain or simply represent non-native structural features elicited by the experimental conditions, we have been prompted to study a longer peptide that, according to a model proposed by Hjorth *et al.* [23], might represent the entire putative el1, residues 88–100. In fact, the additional amino acids are expected to favour the stabilization of the potential conformational features of this region of the receptor.

Although a linear peptide corresponding to el1 is an acceptable model for the loop, a major difficulty, common in the study of the solution structure of peptides reproducing segments of larger molecules is represented by their extensive conformational flexibility. Since this structural status does not necessarily correlate with the degree of freedom of the same segment in the whole protein, cyclization is considered to be a good method to overcome this problem because it restricts the peptide conformational space [48–51].

Here we report a CD and NMR study of a cyclic homologue of el1 (c-el1-KG-NH_2), obtained by coupling the linear peptide to a conformationally restricted template, and its linear form (el1-KG-NH_2), aimed at highlighting the intrinsic structural features of that segment in the AT_{1A} receptor.

MATERIALS AND METHODS

Materials

All protected amino acids as well as the Rink amide MBHA resin were purchased from Calbiochem-Novabiochem (Laufelfingen, CH). Reagents and solvents were purchased from Fluka (Buchs, CH) and used without further purification. HPLC was performed on Waters equipment using column packed with Vydac Nucleosil 300 Å 5 μm C_{18} particles, unless otherwise stated.

Peptide Synthesis and Purification

Peptides were synthesized on a semiautomatic Advanced ChemTech ACT 200 peptide synthesizer using a Rink amide MBHA resin and a standard Fmoc solid-phase peptide synthetic protocol [52–54]. Mass spectra were obtained by electron spray ionization (ESI-MS) on a Finningan MAT SSQ 710C.

Linear peptide *el1-KG*-NH_2: *TAMEYRWPFGNHLKG*-NH_2. The protected peptide [*Fmoc-Thr(tBu)-Ala-Met-Glu(tBu)-Tyr(tBu)-Arg(Pmc)-Trp(Boc)-Pro-Phe-Gly-Asn-(Trt)-His(Boc)-Leu-Lys(Dde)-Gly-resin* was synthesized according to the general procedure. The completeness of each amino acid coupling was verified by the standard Kaiser (ninhydrin) test. After the synthesis, the peptide was cleaved from the resin and the protecting groups were removed. The crude product was purified to homogeneity by preparative reversed-phase HPLC, with final purity greater than 95%, as assessed by analytical HPLC. *m/z* calcd. 1805.05, obs. (ESI-MS) 1806.8 ($M + H^+$), 903.9 ($M + 2H^+/2$), 602.9 ($M + 3H^+/3$).

Cyclic peptide *c-el1-KG*-NH_2 *(Figure 1)*. To ensure a distance between the *N*- and *C*-terminal residues comparable to that in the native receptor [55], an appropriate aromatic spacer was designed.

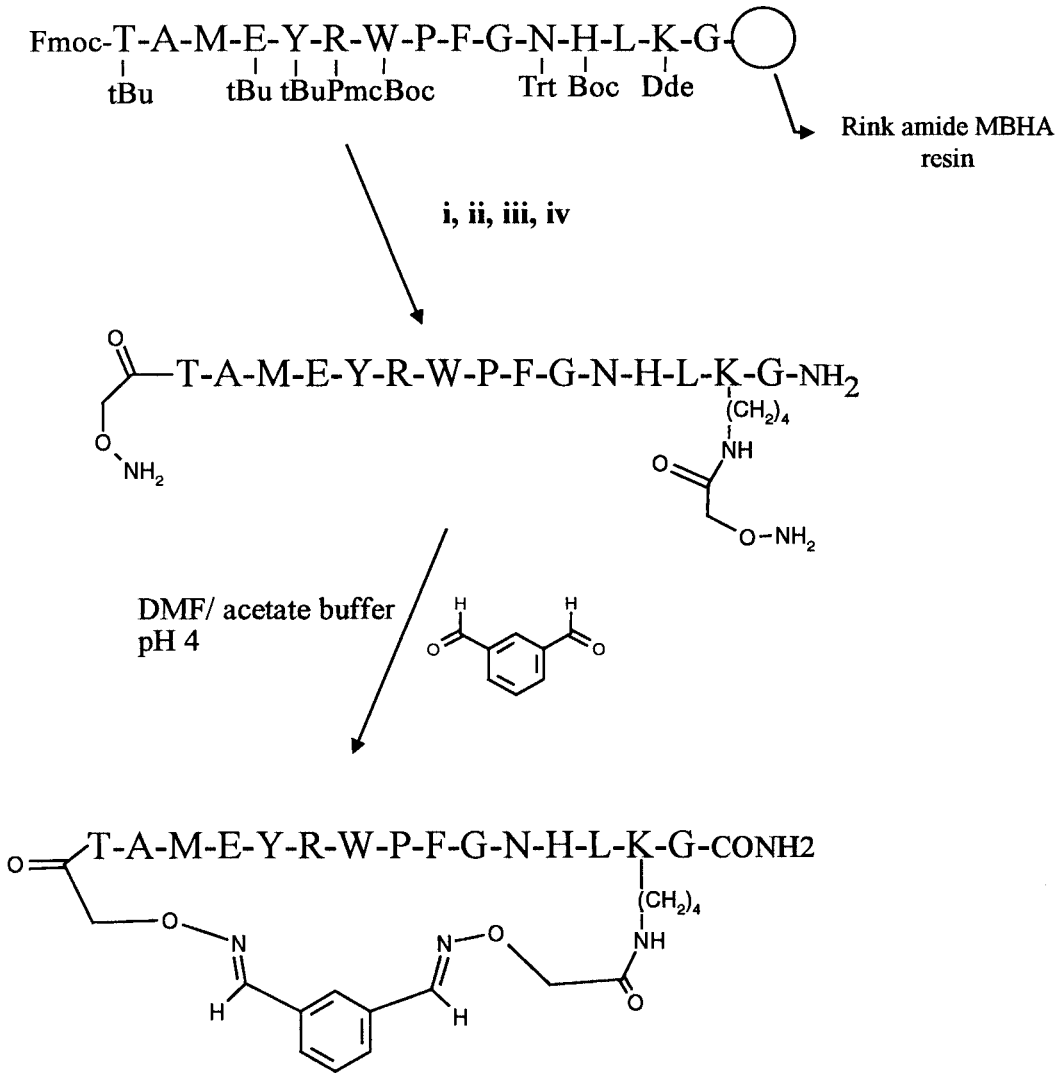

Figure 1 Convergent chemoselective strategy for the synthesis of loop mimetic c-el1-KG-NH_2. **i**. hydrazine (2% v/v in DMF); **ii**. piperidine (20% in DMF); **iii**. Boc-NH-O-CH_2-COOSu (1.5 equiv), DIPEA (3 equiv), DMF; **iv**. 13% (v/v) mercaptoethanol, 2% TIS, 85% TFA.

The synthesis of the cyclic peptide on solid phase was carried out as described for the linear prototype. After deprotection of the α-amino group of the *N*-terminal Thr (20% piperidine in DMF) and of the ε-amino group of Lys (2% hydrazine in DMF), the polymer-bound peptide was condensed with two molecules of the succinic ester of the *N*-Boc-*O*-carboxymethyl hydroxylamine, prepared by adding *N*-hydroxy-succinimide and *N,N*-dicyclohexylcarbodiimide to a solution of *N*-Boc-*O*-carboxymethyl hydroxylamine in a 30 : 70 (v/v) ethyl acetate dioxane mixture. The *N*-Boc-*O*-carboxymethyl hydroxylamine was obtained starting from the commercially available *O*-carboxymethyl hydroxylamine hydrochloride and bis-*tert*-butyl carbonate in a mixture of dioxane/aqueous 0.2 M NaOH (1 : 3). The bis-aminooxy-peptide was then cleaved from the resin and deprotected at the same time using a mixture TFA/TIS/mercaptoethanol (85 : 3 : 12) and, after HPLC purification, dissolved with isophtalaldehyde in a mixture of DMF and aqueous acetate buffer (pH 4.5). A low concentration of the reagents (0.5 mM) was required to favour the intramolecular cyclization of the peptide over the intermolecular condensation. After purification and lyophilization, the compound was authenticated by analytical HPLC. *m/z* calcd. 2049.05 obs. (ESI-MS) 1026.6 ($M + 2H^+/2$), 684.3($M + 3H^+/3$).

The preparative HPLC column (250 × 21 mm) was operated at 18 ml/min, while the analytical column (250 × 4.6 mm) was operated at 1 ml/min, monitoring the absorbance at 214 nm. Solvent A consisted of 0.09% TFA and solvent B of 0.09% TFA in 90% acetonitrile, unless otherwise stated.

Circular Dichroism Spectroscopy

CD spectra were recorded at 25 °C on a Jasco J-715 spectropolarimeter using a Peltier system PTC-348 WVI for cell temperature control. Ellipticity is reported as the mean residue molar ellipticity, [θ] (deg. cm^2 dmol^{-1}). The instrument was calibrated with recrystallized *d*-10-camphorsulfonic acid. The H_2O/TFE and H_2O/MeOH cross-titration experiments were carried out in a 1 mm quartz cuvette mixing the appropriate aliquots of two 0.15 mM stock solutions, one in water and the other in TFE or MeOH. The spectra as a function of pH were obtained on samples in 10 mM buffer: citrate (pH 4), phosphate (pH 6) and borate (pH 8 and pH 10). Each spectrum resulted from the average of five sequential scans. The spectrum of the solvent was recorded under identical conditions and was subtracted. The data were acquired in the spectral range 190–270 nm, using 1 nm bandwidth with a step size of 0.2 nm and a 20 nm/min scan speed.

NMR Spectrometry

NMR samples were prepared in 90 : 10 H_2O/D_2O, pH 4.0, to yield a peptide concentration of 2.4 mM for el1-KG-*NH*$_2$ and 3.0 mM for c-el1-KG-*NH*$_2$. All two-dimensional (2D) ^{1}H-NMR experiments were recorded at 25 °C, using a 5 mm ^{1}H probe-head on Bruker AMX-400 and AMX-600 spectrometers. The chemical shifts were referenced to the H_2O signal located at 4.81 ppm, downfield from DSS. Conventional 2D experiments, such as DQF-COSY [56], TOCSY [57], NOESY [58] and ROESY [59], were used for proton resonance assignments. The TOCSY spectra were acquired using an MLEV-17 [60] spin-lock sequence at a field strength of 10 kHz and an evolution time of 80 ms. NOESY experiments were carried out with mixing times of 150 ms. ROESY spectra were also collected, using a continuous wave mixing of 200 ms (3.0 kHz spin-locking field strength). All 2D experiments were acquired in the phase-sensitive mode using the method of States *et al.* [61], recording 512 t_1 experiments with a variable number of transients of 2048 complex points for each free induction decay. The spectral width in both dimensions was typically 12 ppm. In all spectra, water suppression was achieved by low power continuous-wave irradiation during the relaxation delay, as well as during the mixing time in the case of NOESY experiments. The transmitter offset was placed at the water resonance. Data were processed using the Bruker XWIN-NMR software package. Prior to Fourier transformation, the time-domain data were zero-filled in both dimensions to yield 2K × 2K matrices and apodized by a shifted squared sine bell window function to improve resolution. When required, a fourth-order polynomial baseline correction algorithm was applied after transformation and phasing. Peak-peaking of the transformed spectra was performed using FELIX-97 (Accelrys, San Diego, CA). The cross-peak intensities were measured from the ROESY spectrum for both peptides. To relate the rOes data with the interproton distances, the calibration was made using the distance of 1.8 Å for the well defined geminal β-protons. The rOes intensities were classified as strong, medium and weak, corresponding to upper bound distance constraints of 3.0, 4.0 and 5.0 Å, respectively. Lower bounds between non-bonded atoms were set to the sum of their van der Waals radii (1.8 Å). Pseudo-atom corrections were added to interproton distance restraints where necessary [62]. The ϕ dihedral angle restraints were derived from the $^3J_{HN-\alpha}$ coupling constants, estimated in the 1D spectra whenever possible or in the DQF-COSY spectra [63].

Structure Calculations

The template molecule was built using the Biopolymer module of the InsightII package. The linear peptide was added to the template model. The oximes were forced to be in the more stable E configuration through the simulated annealing protocol tethering the atoms with a template force of 2000kcal/Å^2. All calculations were carried out on a Silicon Graphics O2 workstation using the CVFF [64], implemented in the Discover (Accelrys, San Diego, CA) software package, together with the InsightII program as graphic interface. The structures of the two compounds were computed using the simulated annealing method [65] in the NMR refine module. The simulated annealing calculations included some distinct phases. Phase 1 involved randomization of all atomic coordinates, followed by minimization of the starting structures using a quadratic potential and very low force constants for

each term of the pseudo-energy function, including chiral and NOE constraints. Phase 2 involved simulated annealing with a progressive increment of the force constants up to their full values. Phase 3 involved cooling of the molecule from 1000 to 300 K over 10 ps. At the end of this protocol, the structures were energy minimized with full CVFF (Morse and Lennard-Jones potentials, coulombic term) by steepest descents and conjugate gradients using several thousand iterations, until the maximum derivative was less than 0.001 kcal/Å. Amide bonds were kept in the more stable *trans* conformation. The quality of the final structures was analysed on the basis of the number of rOe distance violations and dihedral angle violations (lower than 0.3 Å and 3°, respectively). Structural analysis was carried out with the program MOLMOL [66].

RESULTS AND DISCUSSION

Peptide Synthesis

To reduce the degree of conformational freedom of the linear peptide and to better mimic the structural restraints present in the native state, the loop was assembled on a template consisting in a partially constrained, aromatic spacer (Figure 1). Its design implied the introduction, at the *C*-terminus of el1, of two additional amino acids, Lys and Gly (el1-KG-NH_2). Lys is required to introduce the hydroxylamino group and Gly is required as a linker to space the Lys residue from the resin and to make its ε-amino group more accessible and reactive. The synthetic strategy adopted for c-el1-KG-NH_2 has its key step in the chemoselective ligation of the unprotected bis-hydroxylamino-peptide with isophthalaldehyde. The two oxime linkages present in the final product were exclusively in the E-configuration, since the Z-configuration is disfavoured by steric hindrance between the oxygen and the aromatic H-2 proton.

Circular Dichroism

The CD spectra of the linear and cyclic peptides have been acquired under various experimental conditions. In aqueous buffer, at pH values ranging from 4 to 10, both peptides show a negative band at ≈200 nm, more intense for el1-KG-NH_2, and a negative shoulder at ≈216 nm (Figure 2). These features are suggestive either of the presence of unordered peptides containing a β-turn [67] or of the coexistence of loose helix, such as the 3_{10}-helix, with unordered segments [68]. In addition, the spectra show a weak positive band at ≈226 nm, again more intense for the linear peptide (Figure 2) and very likely due to the aromatic side chains. For the linear peptide this band is markedly reduced upon increasing the pH from 6 to 8, consistent with a reorientation of the aromatic rings (Figure 2A inset).

Figure 3 shows the CD spectra of both peptides at pH 4 as a function of added TFE. As the TFE concentration increases, various spectral changes are observed for both peptides in the region 195–210 nm indicating the onset of secondary structure elements. In addition, the intensity increase of the negative band at about 216 nm and the corresponding sign variation (from positive to negative) of the 226 nm band (Figure 3 insets) suggest that the acquisition of secondary structure leads to a rearrangement of the aromatic side chains. In both cases, the conformational transition is completed at about 30% TFE (Figure 3 insets).

The dependence of the CD spectra of the two peptides upon added MeOH (Figure 4) has some similarities with the behaviour observed on increasing pH. Upon increasing MeOH concentration, while the intensity of the 200 nm negative band decreases for both peptides, only in the case of the linear peptide is there a concomitant red shift to 204 nm. As in the previous case, an intensity enhancement of the negative band at 216 nm is observed (Figure 4 insets).

Overall, the CD data indicate that the chiroptical activity is higher for the linear peptide than for the cyclic analogue, suggesting that the higher degree of conformational freedom of the former allows the build up of a larger molecular macrodipole. In addition, the shape of the CD profiles supports the hypothesis that the structural organization of the two peptides in aqueous solution and in the presence of MeOH is consistent with either the presence of a β-turn [67] or the coexistence of unordered and loose helix segments [68]. TFE, as expected, induces a stabilization of a conformation with a higher content of helical elements.

NMR

Recognizing that both peptides in aqueous solution exhibit a certain degree of structural organization, their 3D-structure was determined in that solvent. The sequential procedure [62] was used to assign the proton resonances. The corresponding chemical shifts are reported in Tables 1 and 2.

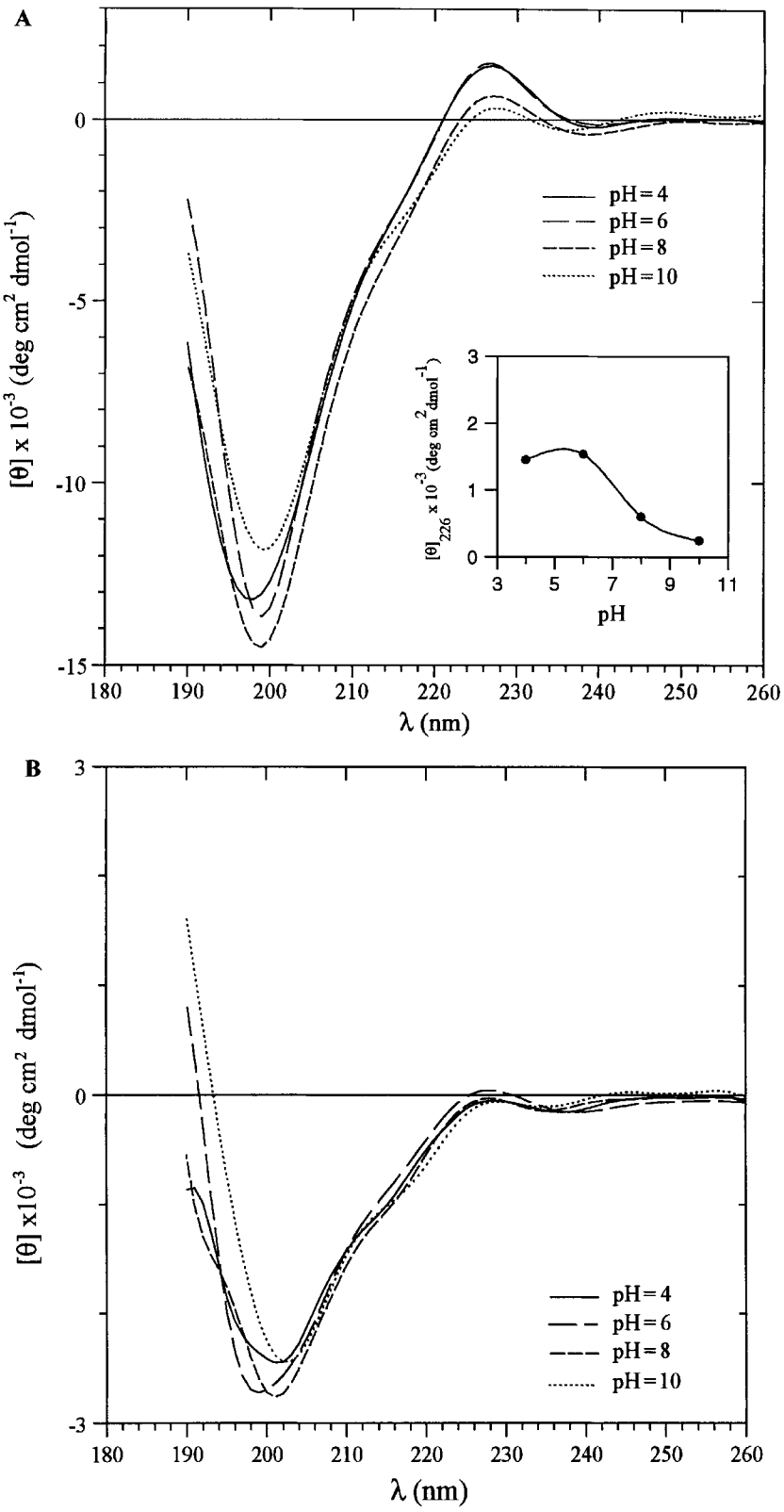

Figure 2 CD spectra of (A) el1-KG-NH_2 and (B) c-el1-KG-NH_2 in aqueous solution as a function of pH at 25 °C. Inset: [θ] at 226 nm as a function of pH.

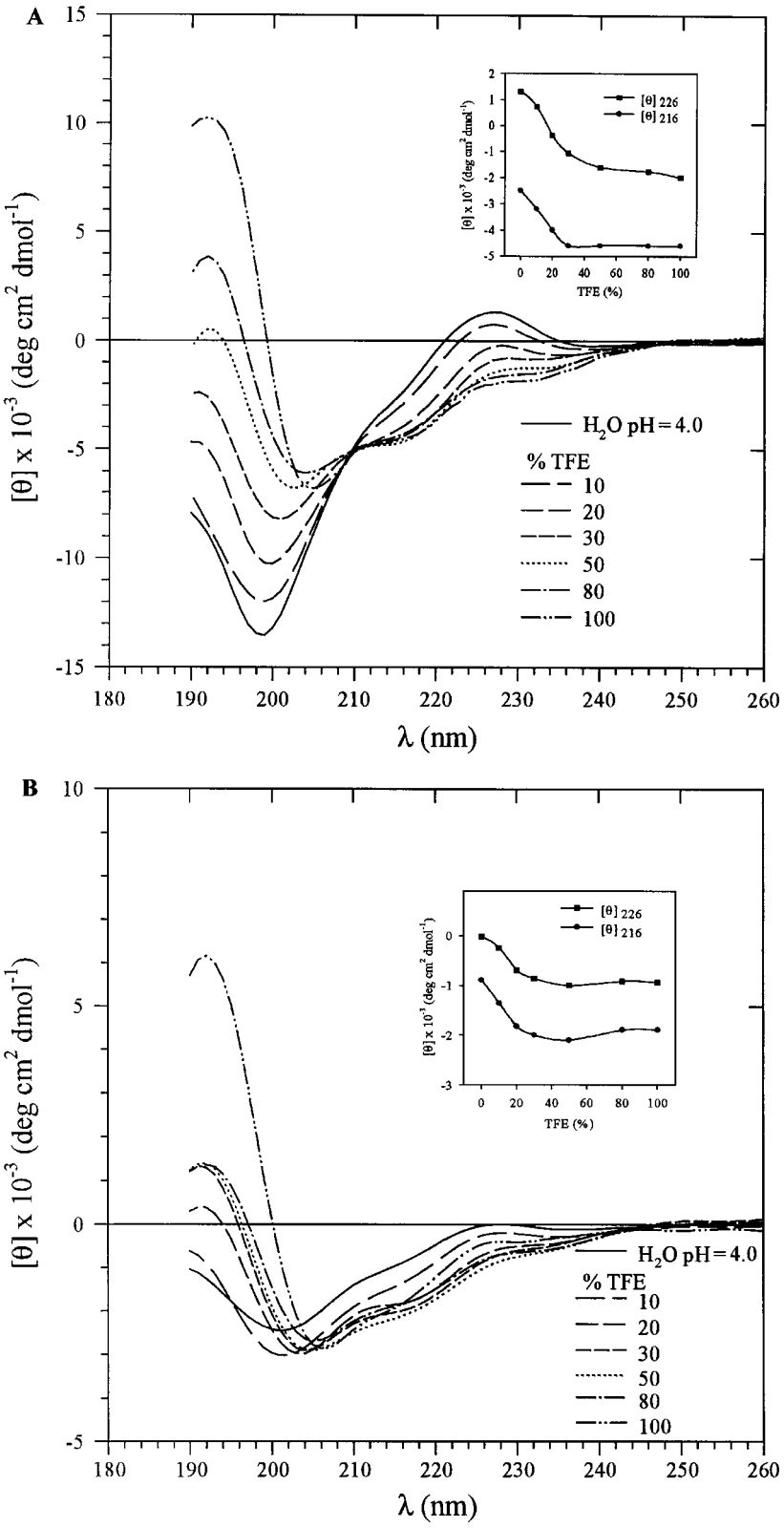

Figure 3 CD spectra of (A) el1-KG-NH_2 and (B) c-el1-KG-NH_2 in H_2O (pH 4.0) upon addition of TFE in the concentration range 0–100% (v/v) at 25°C. Insets: [θ] at 216 and 226 nm as a function of TFE.

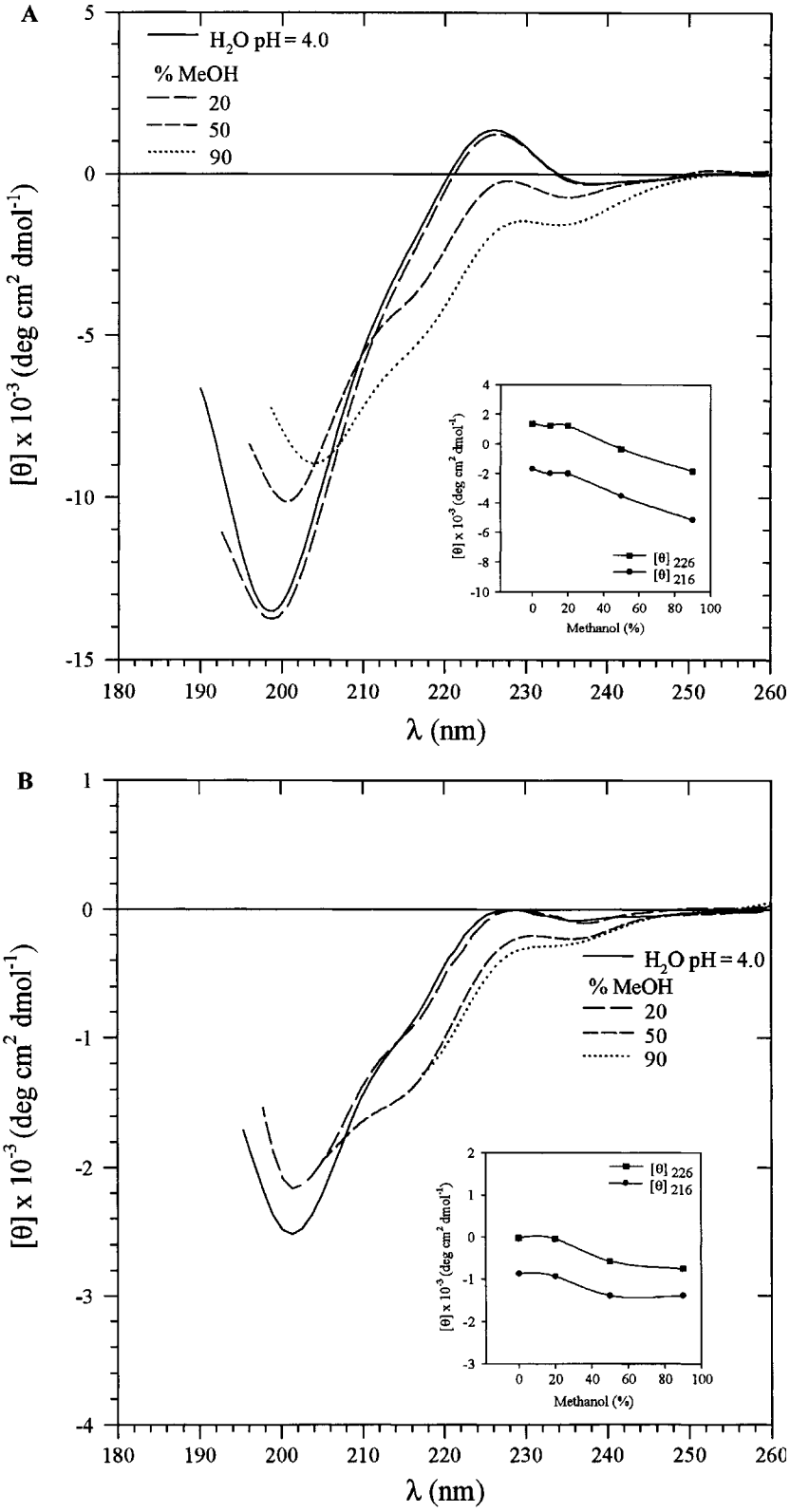

Figure 4 CD spectra of (A) el1-KG-NH_2 and (B) c-el1-KG-NH_2 in H_2O (pH 4.0) upon addition of MeOH at 25 °C. Insets: [θ] at 216 and 226 nm as a function of MeOH.

Table 1 ^{1}H-NMR Chemical Shifts[a] (ppm) and $^3J_{HN-\alpha}$ Coupling Constants (Hz) for the *trans* and *cis*-Pro (in italics) Containing Isomers of el1-KG-*NH*$_2$, in 90% H_2O/10% D_2O, pH = 4 at 25 °C

Residue	$^3J_{HN-\alpha}$	N_H	α_H	β_H	γ_H	Others
Thr[88]			3.90	4.18	1.35	
Ala[89]	5.3	8.85	4.41	1.44		
Met[90]	6.4	8.45	4.40	1.98	2.53	ε_H 1.98
Glu[91]	6.5	8.31	4.27	1.91	2.23	
Tyr[92]	7.0	8.21	4.445	2.835		δ_H 6.97; ε_H 6.69
		8.24	*4.655*	*3.07, 2.88*		*δ_H 7.12*; *ε_H 6.81*
Arg[93]	7.5	7.94	4.22	1.54	1.36	δ_H 3.07; εNH 7.09
		8.165	*4.46*	*1.88, 1.77*	*1.62*	*δ_H 3.23*; *εNH 7.215*
Trp[94]	7.0	8.065	4.93	3.22, 3.09		1NH 10.18; 2H 7.26; 4H 7.71; 5H 7.21; 6H 7.25; 7H 7.47
		8.41	*4.23*	*3.22, 3.13*		*1NH 10.25; 2H 7.24; 4H 7.49; 5H 7.13; 6H 7.24; 7H 7.51*
Pro[95]			4.39	2.14, 1.75	1.91, 1.71	δ_H 3.79, 3.53
			4.17	*1.54, 0.64*	*1.31, 1.12*	*δ_H 3.30, 3.14*
Phe[96]	5.8	7.80	4.67	3.22, 2.95		δ_H 7.19; ε_H 7.37; ζ_H 7.30
Gly[97]		8.25	3.99, 3.85			
		8.23	*3.87, 3.7*			
Asn[98]	7.3	8.27	4.65	2.72		γNH_2 7.50, 6.87
		8.18	*4.64*	*2.71*		*γNH_2 7.54, 6.86*
His[99]	8.0	8.525	4.64	3.23, 3.11		2H 8.505; 4H 7.19
		8.33	*4.475*	*3.21, 3.085*		*2H 8.565; 4H 7.255*
Leu[100]	7.0	8.21	4.33	1.63	1.575	δ_H 0.92, 0.865
		8.26	*4.35*	*1.64*	*1.58*	*δ_H 0.92, 0.875*
Lys	7.2	8.38	4.275	1.82, 1.77	1.42	δ_H 1.69; ε_H 3.00
		8.41	*4.29*	*1.82, 1.77*	*1.42*	*δ_H 1.69*; *ε_H 3.01*
Gly		8.385	3.92			term-NH_2 7.47, 7.09
		8.405	*3.92*			

[a] Chemical shifts are relative to the H_2O resonance, located at 4.81 ppm downfield from DSS.

For both molecules the TOCSY spectra show two distinct sets of resonances for almost each spin system, indicating that a *cis-trans* isomerization at the Trp[94]-Pro[95] peptide bond is operative and affects most of the peptide sequence, as it had been observed for *f*el1 under various experimental conditions [46, 47]. The assignment of the protons corresponding to the two conformers was based on the observation, in the NOESY and ROESY spectra, of the characteristic connectivities between Trp[94]-αH and Pro[95]-αH for the *cis* isomer and between Trp[94]-αH and Pro[95]-δH for the *trans* isomer. Moreover, in the ROESY spectra, exchange cross-peaks between resonances of the two isomers were observed with the same sign of the diagonal, confirming that the two forms are in slow exchange in the NMR time scale. An estimate of the relative resonance intensity indicates that the two isomer forms are present in an approximate *cis-trans* ratio of 1 : 3 for el1-KG-*NH*$_2$ and 2 : 3 for c-el1-KG-*NH*$_2$.

Due to the limited number of well resolved NOESY and ROESY peaks deriving from the *cis* isomers, only the more populated *trans* form was considered for the conformational analysis of the two compounds.

A total of 76 and 67 significant rOe-derived distance constraints together with 9 and 12 ϕ-dihedral angles restraints were measured for el1-KG-*NH*$_2$ and c-el1-KG-*NH*$_2$, respectively. The secondary structure of each peptide was derived from the analysis of the sequential C_αH(i)-NH(i + 1) and NH(i)-NH(i + 1) rOes (Figure 5). The detection, in the ROESY spectra of both peptides, of an intense cross-peak connecting the amide protons of Phe[96] and Gly[97], along with a strong cross-peak between the α-proton of Pro[95] and the amide proton of Phe[96] suggests the presence of a type-II β-turn involving the segment Trp[94]-Gly[97]. Two weak rOe peaks between the α-proton of Pro[95]

Table 2 ^{1}H-NMR Chemical Shifts[a] (ppm) and $^{3}J_{HN-\alpha}$ Coupling Constants (Hz) for the *trans* and *cis*-Pro (in italics) Containing Isomers of c-el1-KG-NH_2 in 90% H_2O/10% D_2O, pH = 4 at 25 °C

Residue	$^{3}J_{HN-\alpha}$	N_H	α_H	β_H	γ_H	Others
Thr[88]	7.7	8.08	4.51	4.36	1.25	
	7.8	*8.06*	*4.49*	*4.36*	*1.25*	
Ala[89]	5.8	8.53	4.20	1.39		
	5.7	*8.48*	*4.19*	*1.38*		
Met[90]	6.8	8.14	4.30	1.96	2.48	ε_H 1.96
Glu[91]	6.9	8.06	4.06	1.87	2.14	
	7.6	*8.09*	*4.18*	*1.88*	*2.15*	
Tyr[92]	7.9	7.81	4.38	2.89, 2.81		δ_H 6.95; ε_H 6.70
	8.7	*7.95*	*4.58*	*3.07, 2.86*		*δ_H 7.05; ε_H 6.74*
Arg[93]	7.9	7.74	4.18	1.55, 1.50	1.29	δ_H 3.00; εNH 7.04
	7.8	*7.87*	*4.45*	*1.88, 1.75*	*1.60*	*δ_H 3.19; εNH 7.18*
Trp[94]	7.0	7.93	4.93	3.19, 3.07		1NH 10.12; 2H 7.20; 4H 7.62; 5H 7.12; 6H 7.18; 7H 7.41
		8.43	*4.65*	*3.22, 3.13*		*1NH 10.24; 2H 7.23; 4H 7.45; 5H 7.11; 6H 7.23; 7H 7.50*
Pro[95]			4.39	2.10, 1.64	1.84, 1.65	δ_H 3.72, 3.44
			4.18	*1.51, 0.53*	*1.27, 1.04*	*δ_H 3.26, 3.09*
Phe[96]	5.7	7.68	4.65	3.22, 2.91		δ_H 7.13; ε_H 7.33; ζ_H 7.26
Gly[97]	11.8	8.24	4.00, 3.83			
Asn[98]	8.7	8.28	4.62	2.75		γNH_2 7.49, 6.86
	7.9	*8.22*	*4.64*	*2.74*		*γNH_2 7.55, 6.85*
His[99]	7.8	8.48	4.58	3.18, 3.09		2H 8.46; 4H 7.12
		8.30	*4.45*	*3.19, 3.08*		*2H 8.52; 4H 7.21*
Leu[100]	7.6	8.17	4.31	1.60	1.54	δ_H 0.89, 0.84
	6.8	*8.24*	*4.31*	*1.61*	*1.55*	*δ_H 0.90, 0.83*
Lys	7.6	8.19	4.09	1.72, 1.60	1.60, 1.27	δ_H1.24; ε_H 3.00
	7.0	*8.21*	*4.13*	*1.75, 1.64*	*1.58, 1.33*	*δ_H 1.24; ε_H 3.01*
Gly	12.5	8.17	3.90, 3.84			term-NH_2 7.41, 7.07
	12.4	*8.21*	*3.90, 3.84*			*term-NH_2 7.43, 7.07*

[a] Chemical shifts are relative to the H_2O resonance, located at 4.81 ppm downfield from DSS.

and the amide proton of Gly[97] for c-el1-KG-NH_2 and between δH-Pro[95] and the amide proton of Gly[97] for el1-KG-NH_2 further confirm the presence of a β-turn.

However, despite these similarities, few important differences are found in the rOe patterns of the two peptides that are related mainly to the residues Tyr[92], Arg[93], Phe[96] and Asn[98]. Indeed, six additional sequential rOe peaks, HN/Tyr[92]-HN/Arg[93], HN/Arg[93]-HN/Trp[94], HN/Asn[98]-HN/His[99], HB/Tyr[92]-HN/Arg[93], HB/Arg[93]-HN/Trp[94], HB/Asn[98]-HN/His[99], are observed only for the linear peptide. The detection of $d_{NN}(i,i+1)$ rOes and their coexistence with $d_{\alpha N}(i,i+1)$ rOes of comparable intensities in the same region (Figure 5) suggests the presence of conformational fluctuations for these residues.

Structure Analysis

The solution structures of the two molecules were calculated following the protocol described in Materials and Methods. Of the 100 computed structures, based on their low residual distance and dihedral angles violations with respect to the experimental constraints, 87 and 86 models were selected, for el1-KG-NH_2 and c-el1-KG-NH_2, respectively. For each peptide a subset containing 50 of the refined structures was randomly selected. These ensembles of structures are shown in Figure 6, where only the segment Tyr[92]-His[99] is displayed for the sake of clarity; in fact, as a result of the paucity of NOEs, the backbone of the remaining part of the peptide exhibits a high disorder in both molecules. As it can be seen, the structure convergence is good for the domain Trp[94]-Gly[97] with the backbone

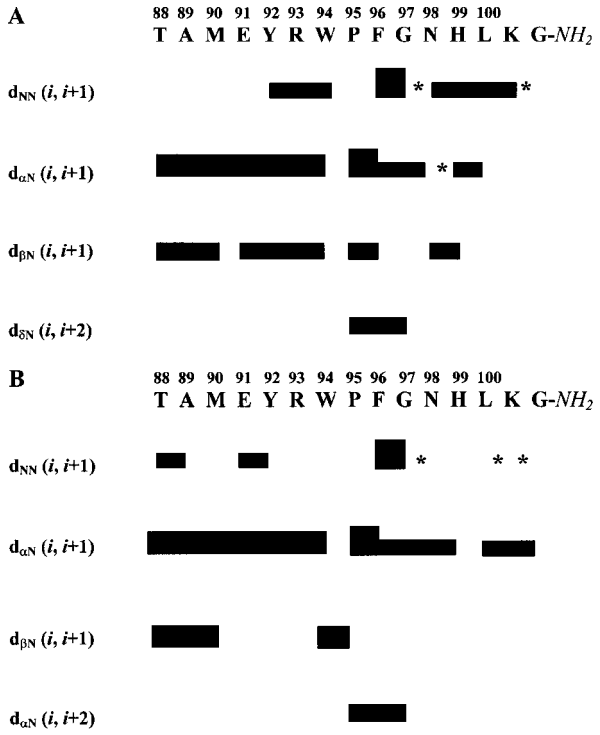

Figure 5 Summary of sequential and medium-range rOes for the *trans*-Pro containing isomers of (A) el1-KG-NH_2 and (B) c-el1-KG-NH_2, in 90% H_2O/10% D_2O, pH = 4 at 25 °C. The thickness of the bars indicates the intensities of rOes classified as strong, medium and weak. An asterisk denotes potential rOe connectivities that could not be observed due to resonance overlap.

atoms showing a root-mean-square deviation (rmsd) with respect to the mean structure of 0.46 ± 0.1 Å and 0.43 ± 0.1 Å for el1-KG-NH_2 and c-el1-KG-NH_2, respectively. For both peptides, the derived ϕ and ψ dihedral angles of this region (Figure 7) are within $\pm 30°$ with respect to the idealized angles for a type-II β-turn, as also suggested by the rOe patterns. In addition, the superposition of the two ensembles of structures (el1-KG-NH_2 *versus* c-el1-KG-NH_2) in the region Trp^{94}-Gly^{97} gives a rather low rmsd value (0.8 Å). This finding, along with the large identity of chemical shifts of their main-chain protons (Tables 1 and 2), confirms that the backbone structural features of that segment are not influenced by the presence of the template. However, it is worth pointing out that in the case of c-el1-KG-NH_2 the template keeps the *N*- and *C*-termini at a distance ranging from 8.1 Å to 13.9 Å (as measured from Thr^1N to $Lys^{14}N\zeta$), with an average value of 10.6 Å, in the ensemble of structures, that is consistent with the expected distance in the whole receptor [55].

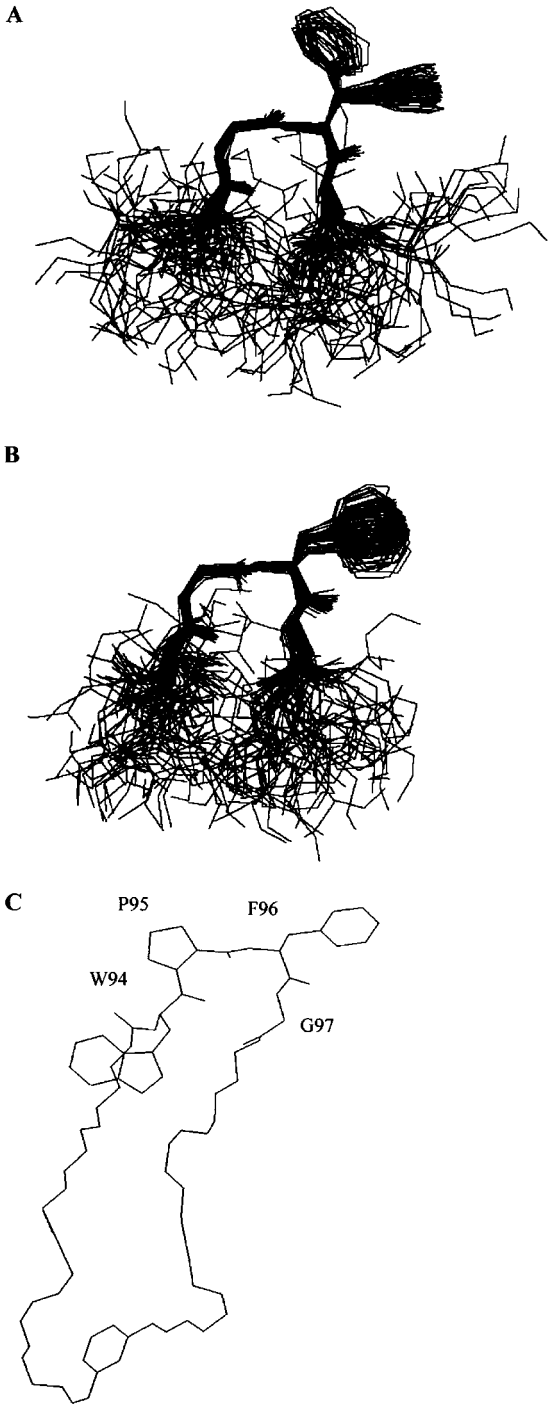

Figure 6 Ensembles of 50 final selected structures of the *trans*-Pro isomers of (A) el1-KG-NH_2 and (B) c-el1-KG-NH_2. Only the segment Tyr^{92}-His^{99} is displayed for clarity; the backbone atoms from residues Trp^{94} to Gly^{97} were used for superposition. The side-chain orientation of Phe^{96} is shown. (C) A representative structure of the peptide c-el1-KG-NH_2 including the spacer; side-chains from Trp^{94} to Gly^{97} are also shown.

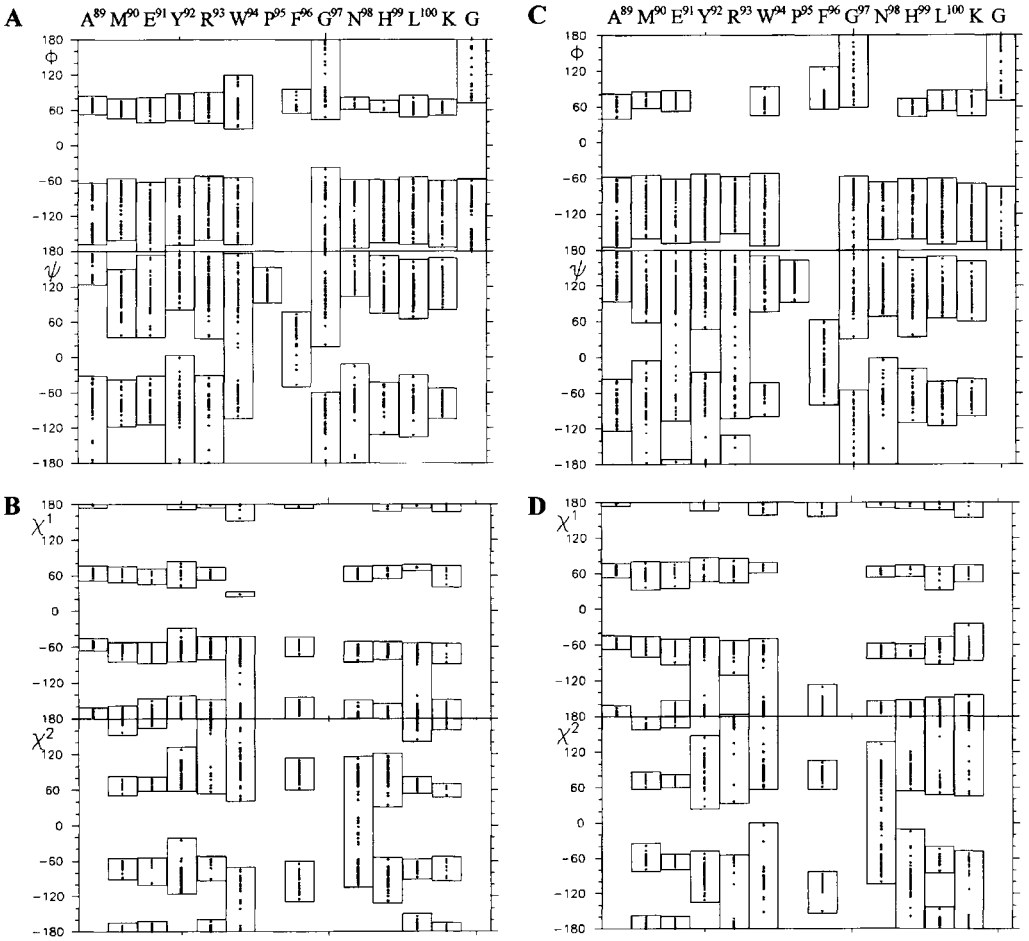

Figure 7 Backbone (ϕ/φ) and side-chain (χ^1/χ^2) dihedral angles distribution as point inside bars for el1-KG-NH_2 (A, B) and c-el1-KG-NH_2 (C, D) final structures.

Interestingly, for the residues Tyr^{92}, Arg^{93} and Asn^{98}, that flank the β-turn, the ϕ/ψ maps (Figure 7) show that in the case of the linear peptide there are two preferential subsets of values, while only one is observed for the constrained homologue. This result suggests that residues not belonging to segments of ordered secondary structure sense the restriction in conformational freedom imposed by the spacer.

As for the side chains, in the case of Phe^{96}, the linear peptide shows two distinct and equally populated values for the χ^1 angle (Figure 6A), roughly with the same potential energy, while in the presence of the template a single orientation is observed (Figure 6B). By contrast, the side chains of Tyr^{92} and Arg^{93} preserve their high degree of conformational flexibility.

Based on these observations, we believe that the type-II β-turn spanning the $W^{94}PFG^{97}$ sequence of el1 as well as the high mobility of the side chains of both Tyr^{92}, suggested to be involved in angiotensin II binding [23–25], and Arg^{93}, may be considered intrinsic conformational features retained in the cognate sequence of the AT_{1A} receptor. Instead, the two possible orientations exhibited by the side chain of Phe^{96} in the linear peptide, since they are not present in the cyclic analogue, very likely can be considered the result of the peptide conformational freedom.

CONCLUSIONS

Taken together, our results indicate that the spacer, while it keeps the *N*- and *C*-terminus of c-el1-KG-NH_2 at an average distance of about 10 Å (Figure 6C), compatible with the value expected for el1 in the whole receptor, does not alter the peptide secondary structure encoded in that amino acid sequence.

On the other hand, the spacer affects some features of the peptide backbone flexibility as well as the preferential orientation of some of the side chains. Indeed, the relative population of the two *cis-trans* isomers, that is approximately 1 : 3 in the linear peptide, increases to 2 : 3 in the cyclic analogue, perhaps as a result of the reduction of the energy difference between the two isomers. Moreover, as shown in Figure 7, the template affects the ϕ/ψ angles of a few residues flanking the β-turn and influences the conformational freedom of the side-chains of the residues close, or belonging to the peptide structural determinant (Figures 6 and 7).

In conclusion, we believe that, when studying isolated segments of large proteins, the introduction of a template, while it favours the stabilization of secondary structure elements encoded in the amino acid sequence, can also be an effective tool to highlight the possible existence of structural features induced by the non-native conformational freedom of the linear form.

Acknowledgements

This work was partially supported by CNR n.99.02608.CT04, MIUR 60% and MIUR Cofin 2001 (A.S.). The Interfaculty Centre for Measurements (CIM) of the University of Parma and the Large Scale Facility for Relaxometry and Magnetic Resonance on Paramagnetic Molecules at the University of Florence are acknowledged for the use of their equipment.

REFERENCES

1. Palczewski K, Kumasaka T, Hori T, Behnke CA, Motoshima H, Fox BA, LeTrong I, Teller DC, Okada T, Stenkamp RE, Yamamoto M, Miyano M. Crystal structure of rhodopsin: a G protein-coupled receptor. *Science* 2000; **289**: 739–745.
2. Kunishima N, Shimada Y, Tsuji Y, Sato T, Yamamoto M, Kumasaka T, Nakanishi S, Jingami H, Morikawa K. Structural basis of glutamate recognition by a dimeric metabotropic glutamate receptor. *Nature* 2000; **407**: 971–977.
3. Henderson R, Baldwin JM, Ceska TA, Zemlin F, Beckmann E, Downing KH. Model for the structure of bacteriorhodopsin based on high-resolution electron cryo-microscopy. *J. Mol. Biol.* 1990; **213**: 899–929.
4. Donnelly D, Overington JP, Ruffle SV, Nugent JH, Blundell TL. Modeling α-helical transmembrane domains: the calculation and use of substitution tables for lipid-facing residues. *Protein Sci.* 1993; **2**: 55–70.
5. Schertler GR, Villa C, Henderson R. Projection structure of rhodopsin. *Nature* 1993; **362**: 770–772.
6. Schertler GF, Hargrave PA. Projection structure of frog rhodopsin in two crystal forms. *Proc. Natl Acad. Sci. USA* 1995; **92**: 11 578–11 582.
7. Baldwin JM, Schertler GF, Unger VM. An α-carbon template for the transmembrane helices in the rhodopsin family of G-protein-coupled receptors. *J. Mol. Biol.* 1997; **272**: 144–164.
8. Unger VM, Hargrave PA, Baldwin JM, Schertler GF. Arrangement of rhodopsin transmembrane α-helices. *Nature* 1997; **389**: 203–206.
9. Pebay-Peyroula E, Rummel G, Rosenbusch JP, Landau EM. X-Ray structure of bacteriorhodopsin at 2.5 angstrom from microcrystals grown in lipidic cubic phases. *Science* 1997; **277**: 1676–1681.
10. Roelz C, Pellegrini M, Mierke DF. Molecular characterization of the receptor-ligand complex for parathyroid hormone. *Biochemistry* 1999; **38**: 6397–6405.
11. Pellegrini M, Bremer AA, Ulfers AL, Boyd ND, Mierke DF. Molecular characterization of the substance P-neurokinin-1 receptor complex: development of an experimentally based model. *J. Biol. Chem.* 2001; **276**: 22 862–22 867.
12. Ji H, Lueng M, Zhang Y, Catt KJ, Sandberg K. Differential structural requirement for specific binding of nonpeptide and peptide antagonists to the AT1 angiotensin receptor. Identification of amino acid residues that determine binding of the antihypertensive drug losartan. *J. Biol. Chem.* 1994; **269**: 16 533–16 536.
13. Schambye HT, Hjorth SA, Bergsma D, Sathe G, Schwartz TW. Differentiation between binding sites for angiotensin II and nonpeptide antagonists on the angiotensin II type 1 receptors. *Proc. Natl Acad. Sci. USA* 1994; **91**: 7046–7050.
14. Schwartz TW. Locating ligand-binding sites in 7TM receptors by protein engineering. *Curr. Opin. Biotechnol.* 1994; **5**: 434–444.
15. Strader CD, Fong TM, Underwood D, Dixon RA. Structure and function of G-protein-coupled receptors. *Annu. Rev. Biochem.* 1994; **63**: 101–132.
16. Baldwin JM. Structure and function of receptors coupled to G-proteins. *Curr. Opin. Cell. Biol.* 1994; **6**: 180–190.
17. De Martino JA, Riper GV, Siciliano SJ, Molineaux CJ, Konteatis ZD, Rosen H, Springer MS. The amino terminus of the human C5a receptor is required for high affinity C5a binding and for receptor activation by C5a but not C5a analogs. *J. Biol. Chem.* 1994; **269**: 14 446–14 450.
18. Flanagan CA, Becker I, Davidson JS, Wakefield I, Zhou W, Sealfon SC, Millar RP. Glutamate 301 of the mouse gonadotropin-releasing hormone receptor confers specificity for arginine 8 of mammalian

gonadotropin-releasing hormone. *J. Biol. Chem.* 1994; **269**: 22 636–2 2641.
19. Huang RRC, Yu H, Strader CD, Fong TM. Localization of the ligand binding site of the neurokinin-1 receptor: interpretation of chimeric mutations and single-residue substitutions. *Mol. Pharmacol.* 1994; **45**: 690–695.
20. Wadsworth HL, Chazenbalk GD, Nagayama Y, Russo D, Rapoport B. An insertion in the human thyrotropin receptor critical for high affinity hormone binding. *Science* 1990; **249**: 1423–1425.
21. Strader CD, Fong TM, Graziano MP, Tota MR. The family of G-protein-coupled receptors. *FASEB J.* 1995; **9**: 745–754.
22. Hunyady L, Balla T, Catt KJ. The ligand binding site of the angiotensin AT_1 receptor. *Trends Pharmacol. Sci.* 1996; **17**: 135–140.
23. Hjorth SA, Schambye HT, Greenlee WJ, Schwartz TW. Identification of peptide binding residues in the extracellular domains of the AT1 receptor. *J. Biol. Chem.* 1994; **269**: 30 953–30 959.
24. Yamano Y, Ohyama K, Chaki F, Guo DF, Inagami T. Identification of amino acid residues of rat angiotensin II receptor for ligand binding by site directed mutagenesis. *Biochem. Biophys. Res. Commun.* 1992; **187**: 1426–1431.
25. Feng YH, Noda K, Saad Y, Liu XP, Husain A, Karnik SS. The docking of Arg2 of angiotensin II with Asp281 of AT1 receptor is essential for full agonist. *J. Biol. Chem.* 1995; **270**: 12 846–12 850.
26. Nikiforovich GV, Marshall GR. 3D Model for TM region of the AT-1 receptor in complex with angiotensin II independently validated by site-directed mutagenesis data. *Biochem. Biophys. Res. Commun.* 2001; **286**: 1204–1211.
27. Boucard AA, Wilkes BC, Laporte SA, Escher E, Guillemette G, Leduc R. Photolabeling identifies position 172 of the human AT1 receptor as a ligand contact point: receptor-bound angiotensin II adopts an extended structure. *Biochemistry* 2000; **39**: 9662–9670.
28. Bergsma DJ, Ellis C, Nuthulaganti PR, Nambi P, Scaife K, Kumar C, Aiyar N. Isolation and expression of novel angiotensin II receptor from *Xenopus laevis* heart. *Mol. Pharmacol.* 1993; **44**: 277–284.
29. Franzoni L, Nicastro G, Pertinhez TA, Tato' M, Nakaie CR, Paiva ACM, Schreier S, Spisni A. Structure of the *C*-terminal fragment 300–320 of the rat angiotensin II AT_{1A} receptor and its relevance with respect to G-protein coupling. *J. Biol. Chem.* 1997; **272**: 9734–9741.
30. Franzoni L, Nicastro G, Pertinhez TA, Oliveira E, Nakaie CR, Paiva ACM, Schreier S, Spisni A. Structure of two fragments of the third cytoplasmic loop of the rat angiotensin II AT_{1A} receptor. *J. Biol. Chem.* 1999; **274**: 227–235.
31. Yeagle PL, Alderfer JL, Albert AD. Structure of the carboxy-terminal domain of bovine rhodopsin. *Nature Struct. Biol.* 1995; **2**: 832–834.
32. Yeagle PL, Alderfer JL, Albert AD. Structure of the third cytoplasmic loop of bovine rhodopsin. *Biochemistry* 1995; **34**: 14 621–14 625.
33. Yeagle PL, Alderfer JL, Salloum A, Ali A, Albert AD. The first and second cytoplasmic loops of the G-protein receptor, rhodopsin, independently form β-turns. *Biochemistry* 1997; **36**: 3864–3869.
34. Yeagle PL, Salloum A, Chopra A, Bhawsar N, Ali L, Kuzmanovski G, Alderfer JM, Albert AD. Structures of the intradiskal loops and amino terminus of the G-protein receptor, rhodopsin. *J. Peptide Res.* 2000; **55**: 455–465.
35. Yeagle PL, Choi G, Albert AD. Studies on the structure of the G-protein-coupled receptor rhodopsin including the putative G-protein binding site in unactivated and activated forms. *Biochemistry* 2001; **40**: 11 932–11 937.
36. Pellegrini M, Bisello A, Rosenblatt M, Chorev M, Mierke DF. Binding domain parathyroid hormone receptor: from conformation to function. *Biochemistry* 1998; **37**: 12 737–12 743.
37. Piserchio A, Bisello A, Rosenblatt M, Chorev M, Mierke D. Characterization of parathyroid hormone/receptor interactions: structure of the first extracellular loop. *Biochemistry* 2000; **39**: 8153–8160.
38. Giragossian C, Mierke DF. Intermolecular interactions between cholecystokinin-8 and the third extracellular loop of the cholecystokinin A receptor. *Biochemistry* 2001; **40**: 3804–3809.
39. Ruan KH, So SP, Wu J, Li D, Huang A, Kung J. Solution structure of the second extracellular loop of human thromboxane A2 receptor. *Biochemistry* 2001; **40**: 275–280.
40. Zhang L, DeHaven N, Goodman M. NMR and modeling studies of a synthetic extracellular loop II of the κ opioid receptor in a DPC micelle. *Biochemistry* 2002; **41**: 61–68.
41. Chung DA, Zuiderweg ERP, Fowler CB, Soyer OS, Mosberg HI, Neubig RR. NMR structure of the second intracellular loop of the α2A adrenergic receptor: evidence for a novel cytoplasmic helix. *Biochemistry* 2002; **41**: 3596–3604.
42. Naider F, Arshava B, Ding FX, Arevalo E, Becker JM. Peptide fragments as models to study the structure of a G-protein coupled receptor: the α-factor receptor of *Saccharomyces cerevisiae*. *Biopolymers* 2001; **60**: 334–350.
43. Katragadda M, Alderfer JM, Yeagle PL. Solution structure of the loops of bacteriorhodopsin closely resembles the crystal structure. *Biochim. Biophys. Acta* 2000; **1466**: 1–2.
44. Katragadda M, Alderfer JM, Yeagle PL. Assembly of a polytopic membrane protein structure from the solution structures of overlapping peptide fragments of bacteriorhodopsin. *Biophys. J.* 2001; **81**: 1029–1036.

45. Yeagle PL, Albert AD. Use of nuclear magnetic resonance to study the three-dimensional structure of rhodopsin. *Methods Enzymol.* 2002; **343**: 223–231.
46. Spisni A, Franzoni L, Sartor G, Nakaie CR, Carvalho RSH, Paiva ACM, Salinas RK, Pertinhez TA, Schreier S. NMR, CD, and molecular modeling studies on the solution conformation of a modified fragment of the first extra cellular loop of the angiotensin II AT_1 receptor. *Bull. Magn. Reson.* 1997; **17**: 151–153.
47. Salinas RK, Shida CS, Pertinhez TA, Spisni A, Nakaie CR, Paiva ACM, Schreier S. Trifluoroethanol and binding to model membranes stabilize a predicted turn in a peptide corresponding to the first extracellular loop of the angiotensin II AT_{1A} receptor. *Biopolymers* 2002; **65**: 21–31.
48. Mutter M, Vuilleumier S. A chemical approach to design template-assembled synthetic proteins (TASP). *Angew. Chem. Int. Ed. Engl.* 1989; **28**: 535–554.
49. Mierke DF, Royo M, Pellegrini M, Sun H, Chorev M. Peptide mimetic of the third cytoplasmic loop of the PTH/PTHrP receptor. *J. Am. Chem. Soc.* 1996; **118**: 8998–9004.
50. Tuchscherer G, Grell D, Mathieu M, Mutter M. Extending the concept of template-assembled synthetic proteins. *J. Pept. Res.* 1999; **54**: 185–194.
51. Peri F, Grill D, Dumy P, Yokokawa Y, Welzenbach K, Wertz-Schmidt G, Mutter M. Assembly of binding loops on aromatic templates as VCAM-1 mimetics. *J. Pept. Sci.* 1999; **5**: 313–322.
52. Fields GB, Noble RL. Solid-phase peptide synthesis utilizing 9-fluorenylmethoxycarbonyl amino acids. *Int. J. Pept. Protein Res.* 1990; **35**: 161–214.
53. Sheppard RC, Williams BJ. Acid-labile resin linkage agents for use in solid-phase peptide synthesis. *Int. J. Pept. Protein Res.* 1982; **20**: 451–454.
54. Chang CD, Meienhofer J. Solid-phase peptide synthesis using mild base cleavage of N^{α}-fluorenylmethyloxycarbonylamino acids, exemplified by a synthesis of dihydrosomatostatin. *Int. J. Pept. Protein Res.* 1978; **11**: 246–249.
55. Joseph MP, Maigret B, Bonnafous JC, Marie J, Scheraga HA. A computer modeling postulated mechanism for angiotensin II receptor activation. *J. Protein Chem.* 1995; **14**: 381–398.
56. Rance M, Sorensen OW, Bodenhausen G, Wagner G, Ernst RR, Wüthrich K. Improved spectral resolution in COSY ^{1}H NMR spectra of proteins via double quantum filtering. *Biochem. Biophys. Res. Commun.* 1983; **117**: 479–485.
57. Braunschweiler L, Ernst RR. Coherence transfer by isotropic mixing: application to proton correlation spectroscopy. *J. Magn. Reson.* 1983; **53**: 521–528.
58. Kumar A, Ernst RR, Wüthrich K. A two-dimensional nuclear Overhauser enhancement (2D NOE) experiment for the elucidation of complete proton-proton cross-relaxation networks in biological macromolecules. *Biochem. Biophys. Res. Commun.* 1980; **95**: 1–6.
59. Bax A, Davis DG. Practical aspects of two-dimensional transverse NOE spectroscopy. *J. Magn. Reson.* 1985; **63**: 207–213.
60. Bax A, Davis GD. MLEV-17-based two-dimensional homonuclear magnetization transfer spectroscopy. *J. Magn. Reson.* 1985; **65**: 355–360.
61. States DJ, Haberkorn RA, Ruben DJ. A two-dimensional nuclear Overhauser experiment with pure absorption phase in four quadrants. *J. Magn. Reson.* 1982; **48**: 286–292.
62. Wüthrich K. *NMR of Proteins and Nucleic Acids*. Wiley: New York, 1986.
63. Kim Y, Prestegard JH. Measurement of vicinal couplings from cross-peaks in COSY spectra. *J. Magn. Reson.* 1989; **84**: 9–13.
64. Dauber-Osguthorpe P, Roberts VA, Osguthorpe DJ, Wolff J, Genest M, Hagler AT. Structure and energetics of ligand binding to proteins: *E. coli* dihydrofolate reductase-trimethoprim, a drug-receptor system. *Proteins: Struct. Funct. Genet.* 1988; **4**: 31–47.
65. Nilges, M, Clore GM, Gronenborn A. Determination of three-dimensional structures of proteins from interproton distance data by dynamical simulated annealing from a random array of atoms. *FEBS Lett.* 1988; **239**: 129–136.
66. Koradi R, Billiter M, Wüthrich K. MOLMOL: a program for display and analysis of macromolecular structures. *J. Mol. Graphics* 1996; **14**: 51–55.
67. Urry DW. Characterization of soluble peptides of elastin by physical techniques. *Methods Enzymol.* 1982; **82**: 673–717.
68. Toniolo C, Polese A, Formaggio F, Crisma M, Kamphuis J. Circular dichroism spectrum of a peptide 3_{10}-helix. *J. Am. Chem. Soc.* 1996; **118**: 2744–2745.

